FINDING ANSWERS IN STARLIGHT

Abigail Huang, Shankar Iyer, Minyoung Jang, Chang Kim, Victoria Lent, Elise Pasoreck, Sheila Prakash, Mark Saigh, Douglas Swanson, Gary Yen

Advisor: Dr. Keith Andrew
Assistant: Karen Mooney

ABSTRACT

The analysis of starlight can reveal information about the universe around us. The team project in astrophysics utilized the Drew University telescope and CCD camera technology to collect data about various celestial objects. We observed the globular cluster M13 in order to calculate the age of the Milky Way galaxy. In an effort to compute the upper limit of Einstein's cosmological constant, we measured the angular velocity of Pluto. We also searched for quasars, arguably the most baffling objects in the universe. Lastly, we obtained the absorption spectrum of the star Vega and determined its elemental components.

INTRODUCTION

For as long as humans have been able to ask questions, they have possessed innate desires to understand the world around them. The cosmos, though, proved challenging to human comprehension for many centuries. The earliest astronomers were unable to obtain clear pictures of most celestial objects. Thus, they proposed various hypotheses explaining what they were able to view through their crude instruments. Now, with the advent of modern technology, we are able to answer many of these early astronomical questions.

EQUIPMENT

Hardware

Our data was primarily collected using a 0.41m (16 inch) f/8 Ritchey-Chrétien automated reflecting telescope, manufactured by DFM Engineering Inc., as well as a CCD camera. [1]

The number F/8 means that focal length is 8 times the diameter of the lens and describes how bright objects viewed through the telescope will be. Although different kinds of objects are viewed best under different f/ratios, F/8 is a midrange number and works fairly well with most objects. [2]

Figure 1: A coma "stretches out" or distorts the image

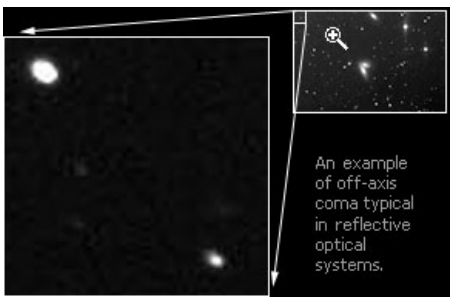

Ritchey-Chrétien refers to a specialized correction lens on our telescope. Most reflecting telescopes have an aberration called coma (see image left), which this lens fixes. Also notable is that the RC design has no refractive elements, whereas glass lenses scatter light, especially in infrared (IR)

range where CCD cameras are most sensitive. Therefore, the RC lens is critical for CCD photography, where a large aberration-free field of view is required. [3]

We used two cameras to take images: the ST-10XE and the ST-8E, both manufactured by the Santa Barbara Instrument Group. Due to its larger field of view, the ST-10XE was used to take more general images of the night sky. However, this camera also had lower resolution capabilities, so for more detailed pictures the ST-8E was used [4]. This was also the camera that fit the spectrometer and filter wheel, so images that required the use of these pieces of equipment were taken with this camera.

A CCD (charged coupled device) is a chip that converts the light that reaches it into proportional analog signals [5]. The ST-8E contains two of these chips used together, one for imaging and the other for tracking. This makes it more efficient in collecting images, and the additional chip allows increased accuracy in locating the objects to be photographed. The ST-10XE contains only one chip.

In order to minimize distortion due to high temperatures, the cameras are also equipped with cooling units that bring their temperatures down to about -5ºC.

To filter various wavelengths of collected starlight, Bessel Photometric Filters, manufactured by Omega Optical Incorporated, were used. These instruments are coated to prevent reflection, and contain two to three Schott filter glasses, each created to conform to strict thickness regulations [6]. Each filter glass is intended to segregate a specific wavelength of the electromagnetic spectrum, and filters for ultraviolet, blue, green, red, and visible wavelengths were employed in this experiment [7].

For quicker movement between wavelengths being isolated, the filters were encased in a CFW-8A wheel purchased from Santa Barbara Instruments Group. Positioned between the viewing lens of the telescope and the camera, this instrument may be operated through the CCDOPS software. Photos taken through the wheel are also processed using the same program [8].

The Self Guided Spectrograph or SGS is a device that can be attached to the telescope camera to obtain the spectral lines of a celestial object. The SGS works on the basic principle of photon absorption and emission by atoms. The collected light first passes through a narrow slit on the lens of the SGS to limit the amount of light entering the device. The light then passes through a prism inside the SGS, and the various wavelengths of light are then separated into a spectrum band. This spectrum is captured by a camera and transferred to the CCDOPS program. The spectrum can then be displayed and manipulated using the computer. On the bottom of the SGS is a frosted glass lens used to take a calibration spectrum. If the star and calibration spectrum are simultaneously taken with the two lenses, the star's spectrum is superimposed on the middle third of the calibration spectrum [9].

Software

When used in conjunction with the telescope and when used independently, TheSky

Software allows for access of star maps with celestial objects covering several databases. These include the Hubble Guide Star Catalog, the Hipparcos/Tycho Stellar Catalog, and the Catalog of Galaxies and Clusters of Galaxies [10]. In total, TheSky can locate over 15 million stellar objects and 4 million non-stellar objects. After searching for a specific object to view, the user receives information concerning that object's location in the sky and its magnitude. These figures proved useful in the selection of reference stars, or stars of known magnitude, which could then be used to calculate the magnitudes of other stars in a photograph [11].

TheSky was also vital in the collection of the photographs themselves. Linked to the telescope, TheSky software directs the slewing of the telescope in the observatory in preparation for the acquisition of images by the camera. This feature, though inhibited by a slight error in the accuracy of the slewing, was imperative to the retrieval of raw data [11].

Effective use of the program was often hindered by the necessity of the knowledge of the name of an object prior to undertaking a search [11]. Often cognizant of the coordinates of an important celestial body, we would need to employ the Palomar or Redshift software along with The Sky to find the desired object.

RealSkyView software contains the Digitalized Sky Survey, an image catalogue compiled from the Palomar Observatory Sky Survey. This program allows the user to locate a target object recorded in the New General Catalog, among other databases. An object can either be located by searching for it by name, or by entering known right ascension and declination coordinates of the object and angular dimensions of the sky to display.

For this project, RealSky was most frequently used to locate reference stars and their coordinates to match up experimental photographs with standard database images. RealSky also can find the orientation of an image or find the centroid of a set of target objects, both useful features in comparing and identifying multiple images.

Redshift is a multimedia astronomy program that allows the user to view the sky via actual location and time. One can identify an object in the field of view by clicking on it. A box displaying the desired object's proper name, coordinates, visual magnitude, and distance from the viewing location will appear on the screen. For the quasar project, Redshift was used to find reference stars within close proximity to the chosen quasars.

The CCDOPS program is used to interface the Santa Barbara CCD camera with the observatory computer to focus the camera and photograph the target object the telescope is centered on. The CCDOPS program is also responsible for controlling the cooling of the camera, which is necessary to reduce the light noise picked up by the camera to obtain a better image. The program can perform the subtraction of dark frame from light frame automatically (see procedure below).

We used the MIRA Pro and MIRA AP computer programs, version 6, to analyze and process the images received from the camera and telescope system. MIRA enabled our team to subtract dark frame and flat frame images from our pictures, which dramatically improved the quality of the images by eliminating impurities due to the telescope apparatus and CCD camera

chip. MIRA also allowed us to scale, rotate, and crop images. We could align sets of images by performing both rotational and direct coordinate transformations, and we could also filter images using various techniques. MIRA had the ability to calculate the center of mass of an image, or to convert an image file from one format to another. It cycled through images in a set in order to search for asymmetries or aberrations. Lastly, MIRA contained aperture photometry operations to compute relative magnitudes of stars and other stellar phenomena given a reference point of known magnitude.

Spectra Analysis Software is a graphical analysis program used to map known wavelengths onto an unknown spectrum. An unknown and a known calibration spectrum are simultaneously displayed on screen, making it possible to identify the spectral lines of the unknown sample by corresponding them by intensity, width, and location of the lines on the known sample. Once the two lines are correctly identified and labeled with a wavelength, the program allows the user to determine the wavelength and intensity of any line on the unknown spectrum [9].

MatLab is a mathematics package which generates high-resolution graphs from entered spectrum data. MatLab provides the user with the ability to zoom in closely on the graph, thus yielding accurate data readings of the spectra [12].

Mathematica is a program used for various mathematical computations. Its most common uses in our project involved data plotting and curve fitting.

Microsoft Excel was used primarily to plot data and create preliminary graphs of this data. Data could be entered into a spreadsheet and later converted to a graph or chart for ease of viewing and comprehension.

BASIC PROCEDURE

At the onset of each experiment, the observatory was prepared with the telescope linked to a computer in the control room as well as two computers in the dome itself. One of the latter machines ran TheSky, the program through which objects were selected for viewing. After the telescope was slewed to the desired celestial body through the same software, a hand control was used to rotate the dome to the necessary position and to select the optimum focus.

The camera, replacing the eyepiece on the telescope, could now begin taking pictures. For selection of exposure times, CCDOPS was used. These periods generally ranged from 0.12 to 120 seconds and were selected based on the brightness of the object. CCDOPS also was used at this time to select the picture type. Taken without any special alterations, light exposures served as the standard photographs; taken with the camera shutters closed, dark exposures were used to capture defects in the CCD chip; taken prior to the emergence of any objects in the night sky, flat field exposures allows for correction of any unnecessary or non-uniform change in the background of the light image. The grab option in CCDOPS finally began the actual photography after the aforementioned selections were completed.

GLOBULAR CLUSTERS

One of the objectives of this team project was to calculate the age of our galaxy, the Milky Way, by analyzing the magnitudes of various stars at different wavelengths within a globular star cluster. When the galaxy was first created, there were small balls of gas that remained separate from the majority of the galaxy's mass. As the galaxy developed and then cooled, these other gaseous regions formed clusters of their own. Therefore, the globular clusters found within the Milky Way are approximately the same age as the galaxy itself.

The Hertzsprung-Russell (HR) diagram is commonly used to determine the age of a cluster of stars. Usually, the graph is a scatter plot of temperature (in kiloKelvins) vs. luminosity (in watts or in units of the sun's luminosity), where each star in the cluster is represented by a single point on the graph. Most of the stars will fall onto a smooth curve known as the Zero Age Main Sequence (ZAMS) curve (see Figure 1 below), but some will diverge. By determining the temperature at the turning point, we can use a computational model to calculate the age of the cluster (see below).

Figure 2: Hertzsprung-Russell diagram [13]

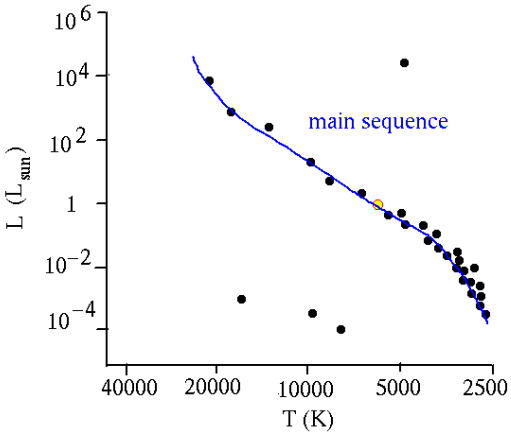

Determining the age of the cluster based on the temperature is rooted in the concept that bigger stars are brighter and hotter. These more massive stars, as a result, consume fuel at a faster rate and move off the ZAMS curve faster than the smaller, dimmer ones. Therefore, the location of the turning point on an HR diagram illustrates how much the cluster has evolved. One instance of this is when smaller, cooler stars are seen moving off the curve—and consequently the cluster is defined to be very old, since it takes longer for those smaller stars to consume all their fuel.

In order to analyze our globular cluster, M13, with the equipment available, we had to make an alternative version of the HR diagram—we needed to plot the visible magnitude against the color index, which in our case was the difference of the blue magnitude and the visible magnitude for each star. The color index and temperature are directly related, so in the end, both graphs looked identical.

Thus, unfiltered pictures, as well as pictures filtered through visible and blue filters, were

taken. Within the MIRA program, a reference star of known magnitude is needed to relatively calculate the magnitudes of other stars in the picture. TheSky provided the visible and blue magnitudes of certain stars near M13, the photographed cluster. As reference stars for each filtered image were then known, these could be employed to determine the visible and blue magnitudes of all other stars in the picture.

An HR diagram was next produced using Excel. If the points were ideal, Mathematica should next have been used to curve fit a ZAMS curve as well a curve of divergent points from that curve. Our data however could not be curve fitted to produce a logical turning or intersection point. Instead of using the conventional method, we therefore were required to select a range of possible turning points. The color indexes of the upper and lower bounds of this range were then placed into the following equation to determine the surface temperatures of their respective stars.

$$T = (12.88)(CI+1)^{-1.61} \text{ kilo} - \text{Kelvins} \quad \text{(Equation 1)}$$

Each of the resulting values were converted to Kelvins and used in the following function for the age of the cluster:

$$t_{age} = (3.9801 \times 10^{28})T^{-4.93} \text{ years} \quad \text{(Equation 2)}$$

The fifty points which we analyzed produced the following HR Diagram:

Figure 3: Visible Magnitude vs. Color Index of Stars in M13

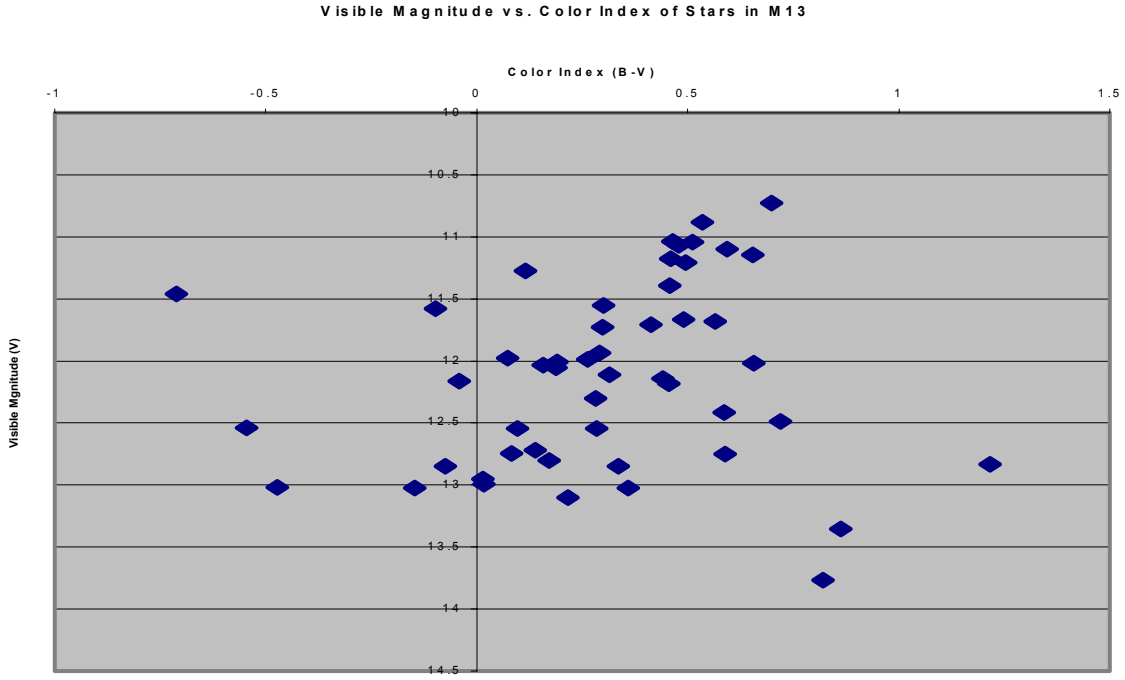

When this data was curve fitted, the resulting intersection points seemed visually incorrect and also resulted in the galaxy being estimated as older than the universe or younger than the Earth. We reasoned that this was due to our use of only fifty points, in turn caused by the fact that our equipment could not photograph dimmer stars. Thus unable to use more accurate methods, we selected a range of possible turning points and used the bounds to approximate an age range for the cluster.

Using a color index range of .2 to .5 and working with Equations One and Two, we calculated that M13, and therefore the Milky Way, is between 926 million and 5.44 billion years. The former of these numbers is also illogical; however, the upper bound is considered to be in the expected range, with error, for the age of the Milky Way galaxy.

PLUTO AND THE COSMOLOGICAL CONSTANT

If one were to take a substantial chunk of the known universe and remove from it every conceivable trace of matter and radiation, a vacuum would result. This vacuum would theoretically contain the lowest energy density of any state, although there is no proof that this value is zero. In General Relativity, any form of energy influences the gravitational field and consequently the dynamical history of the universe, making the vacuum energy density a fairly important term. Since relativity theory did not support a static and unchanging universe, a cosmological constant, denoted by the Greek letter Λ, was incorporated in 1917 by Albert Einstein to serve as a form of "antigravity." This constant had a negative magnitude, and counterbalanced the positive acceleration of General Relativity, making the net acceleration of the universe zero. Later deemed the famous "fudge factor," this constant was a universal number that represented the vacuum energy density found throughout the universe. In 1929, Hubble discovered the red shift of distant galaxies, which proved the universe is expanding. Einstein then abandoned the cosmological constant, declaring it to be the "greatest blunder of [his] career." However, recent research has shown that a cosmological constant may indeed exist, though its value appears to be positive, not negative, and has the effect of accelerating the universal expansion even more than General Relativity predicted.

According to the Einstein field equations, if the entire mass density of the universe is due to the vacuum energy density, the gravitational field is in the form: $G(r)= 4\pi\rho vr/3$ at a distance of r from the Sun. Since the term is directly proportional to the vacuum energy density, the most obvious effects would occur at the most distant planet from the sun, namely, Pluto. Using Kepler's Third Law to eliminate r and neglecting the mass of Pluto, one could use the equation $\Lambda < (3G/c^4)(\omega^2)$ and the angular velocity of Pluto (ω) to place an upper bound on the value of the cosmological constant. In this particular experiment, a value for Pluto's orbital angular velocity was obtained by calculating the angular distance Pluto traveled over a two week surveillance period at the observatory.

In order to obtain a value for Pluto's angular velocity, our team used the telescope and camera apparatus to take several pictures of the planet. After taking the exposures, we analyzed the images using the MIRA computer program. We filtered the images and removed much of the extra "noise" and background radiation. Since the exposures had been centered on Pluto, which moves throughout the sky, the pictures were off-center and disoriented. So, we utilized

the MIRA software to align and rotate the images so that the stars, whose placement is invariant, lined up. Thus, the newly-aligned pictures showed only the movement of the planet Pluto.

With the clear, aligned images, we calculated the angular velocity of Pluto over the specific time periods. We measured the distance (in linear units) between two stars of known angular displacement, and thus generated a conversion factor from linear to angular distances. Then, we measured the motion of Pluto through the various images, and converted the resulting distances to angular displacements. Using those angular displacements, and the known time intervals between the exposures, we calculated the angular velocity of Pluto, which should be approximately constant. Then, we computed the upper limit for the cosmological constant as described in the above procedures.

Table 1: Observational Data for Exposures

Date	Time	Exposure (sec)	Focus	Temperature (°C)
7/31/02	9:12 PM	5	2042	-3.57
8/01/02	9:28 PM	4	2042	10.24
8/03/02	10:09 PM	15	2042	-3.57
8/06/02	9:24 PM	5	2023	-9.79

Each exposure of Pluto (shown in Figures 1 and 2 below) was taken under slightly different conditions. Exposure time affects the appearance of the photograph; the longer the exposure, the more light is collected by the camera, so the stars appear brighter. Fainter stars are visible in longer exposures that are not for shorter exposure times. This explains the appearance and disappearance of some of the fainter stars in the series of Pluto photographs. Exposure time could not always be held constant; rather, it had to be modified to fit experimental factors such as weather and time. The reference stars used, however, are present in all images. The focus of the CCD camera is usually set at a standard of 2042, but it can be modified to match trial conditions in order to obtain sharper images. The temperature of the CCD camera also is a large factor in the clarity of the images, as temperature fluctuations create background noise that obscures the image.

Table 2: Experimental Data for Exposures

Exposure Number	Date	Time	x-Coordinate of Pluto (mm)	y-Coordinate of Pluto (mm)
1	7/31/02	9:12:24 PM	13.356	12.876
2	8/1/02	9:28:42 PM	14.292	12.756
3	8/3/02	10:09:15 PM	16.020	12.636
4	8/6/02	9:24:17 PM	18.372	12.564

We calculated the linear distance, in millimeters, between two known stars, GSC 5651:1585 and GSC 5651:1725, by measuring their x-coordinates and y-coordinates. We used this data to find the change in the x and y coordinates, and computed the linear distance between the stars with the geometric formula as shown:

$$\Delta s = \sqrt{(\Delta x)^2 + (\Delta y)^2} \quad \text{(Equation 3)}$$

Table 3: Data for Calibration Stars

Star	x-coordinate (mm)	y-coordinate (mm)	Δx (mm)	Δy (mm)	Δs (mm)
GSC 5651:1585	19.476	22.356	0.144	1.440	1.447182
GSC 5651:1725	19.620	23.796			

We then equated the linear distance between the stars, 1.447182 mm, with their known angular displacement of 56 arc seconds. Thus, we derived the linear-angular conversion equation:

1.447182 mm = 56 arc seconds (Equation 4)

We calculated the linear distance between the various exposures of Pluto in the same manner, and then converted those distances to angular displacements:

Table 4: Linear and Angular Displacement of Pluto

Exposure Interval	Δx (mm)	Δy (mm)	Δs (mm)	Angular Displacement (arc seconds)
Exposure 1 to Exposure 2	0.936	0.120	0.943661	36.516
Exposure 2 to Exposure 3	1.728	0.120	1.7321697	67.028
Exposure 3 to Exposure 4	2.352	0.072	2.3531018	91.055

We then changed the angular displacement values from arc seconds into radian measures (θ) using the following conversion method:

Arc seconds x (1 arc minute / 60 arc seconds) x (1degree / 60 arc minutes) x
(2π radians / 360 degrees) = Radians (Equation 5)

We also found the time elapsed between each set of exposures in seconds, and then calculated the angular velocity of Pluto (ω) using the following equation:

$$\omega = \Delta\theta / \Delta t \quad \text{(Equation 6)}$$

Thus, we obtained the following values for angular displacement and velocity of Pluto:

Table 5: Angular Displacement and Velocity of Pluto

Exposure Interval	Angular Displacement (arc seconds)	Angular Displacement (radians)	Time Interval (sec)	Angular Velocity (radians/sec)
Exposure 1 to Exposure 2	36.516	1.771×10^{-4}	87378	2.027×10^{-9}
Exposure 2 to Exposure 3	67.028	3.250×10^{-4}	175233	1.855×10^{-9}
Exposure 3 to Exposure 4	91.055	4.415×10^{-4}	261898	1.686×10^{-9}

Taking the average value of our results, we obtained:

$$\omega_{avg} = 1.856 \times 10^{-9} \text{ radians/sec}$$

Using the average value for Pluto's angular velocity, we calculated the upper limit of the cosmological constant, Λ, as follows:

$$\Lambda < \frac{3G}{c^4}\omega^2 \quad \text{(Equation 7) [14]}$$

$$\Lambda < 8.51 \times 10^{-62} \text{ rad}^2/\text{kg}$$

By substituting the average calculated angular velocity (ω) of Pluto into Equation 5, we were able to obtain a value of -8.510×10^{-62} as the upper limit for the cosmological constant. In theory, since the energy density of the universe is a property of spacetime itself, it should remain uniform everywhere. A positive numerical value for the constant would imply that the galaxies are in effect accelerating away from us faster than the initial predictions of general relativity. A zero value would represent a universe that accelerates solely in accordance with general relativity, while a negative value would represent a static universe. Our positive result implies that the universe is expanding with a rapid acceleration.

With this value for Einstein's cosmological constant, we predicted a change in the behavior of the planet Mercury as it orbits the Sun. The cosmological constant should influence the perihelion location of Mercury's orbit by a factor of:

$$\Delta = \pi \frac{\Lambda a^3 \left(1 - e^2\right)^3}{m} \quad \text{(Equation 8) [15]}$$

where *a* denotes the length of the semi-major axis of the elliptical orbit, *e* denotes its eccentricity, and *m* represents the mass of the Sun. Inserting the values into this equation, we obtained a value for Δ of 2.289×10^{-59}. Unfortunately, this discrepancy in Mercury's orbit is far too small to detect by any experimental means, because it represents less than 1 percent of the shift in perihelion location already predicted by Newtonian physics and general relativity. The

cosmological constant's impact falls well within the margin of error of any possible measurement.

Figure 4: Pluto on 7/31/02

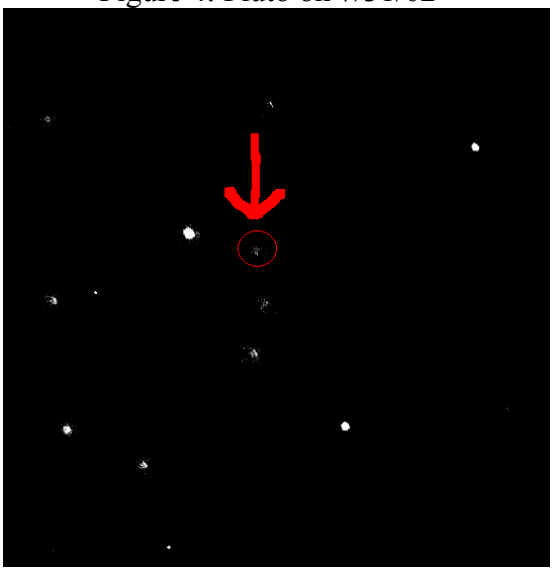

Figure 5: Pluto on 8/6/02

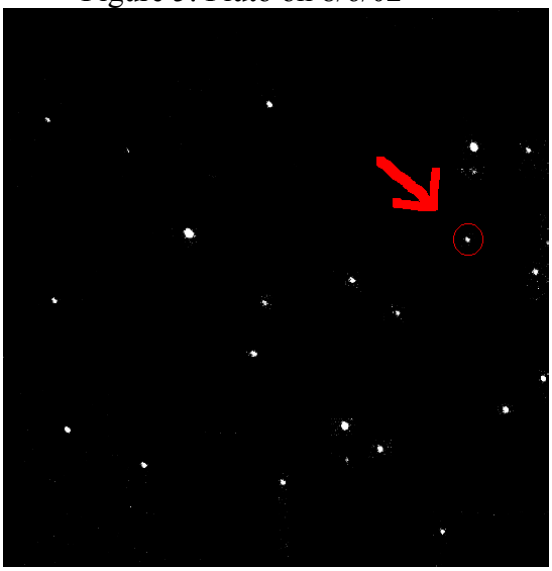

QUASARS

First discovered in 1963, quasi-stellar radio sources, more commonly known as quasars, are considered the most energetic and enigmatic objects in the universe. Despite their relatively compact size (approximately that of our solar system), quasars may emit 10 to 1000 times the energy of the entire Milky Way Galaxy [16]. Although quasars exist at distances of 240 Mpc to 4700 Mpc from Earth, they can be viewed because of their exceptional luminosity. Quasars are such remote objects that we are seeing them as they existed 0.1 to 8.7 billion years ago. Thus, they may offer us a peek at the formative years of the universe.

To date, several theories concerning the composition and luminosity of quasars have been formulated. The most widely accepted theory indicates that quasars are a type of energetic galactic objects known as active galaxies [17]. This theory has some merit, as both quasars and active galaxies possess common features, including high luminosity, non-thermal emissions, jets of luminous matter, and modest size [18].

There are problems, however, relating to the theory that quasars are a type of active galaxy. Since many quasars are so bright, the light of their host galaxies cannot be distinguished sufficiently. Moreover, new evidence of "naked quasars" suggests that quasars are the result of collisions involving independently existing black holes and galaxies [19].

Quasars are thought to receive their power via the accumulation of infalling matter into centrally located supermassive black holes [19]. As the matter spirals into the black holes, part of it is converted to energy and radiated away before the remainder of the mass crosses the event horizon. This phenomenon explains the great luminosity of quasars.

Unfortunately, this model of the quasar is not perfect. Assuming that a quasar consumes 1000 suns a year and that it has been in existence since the beginning of the universe, the black hole at the center of the quasar should have a mass equal to that of 10^{13} suns. This is unlikely, considering that a galactic object containing mass on that order has never been identified. It can then be inferred that rather than actually consuming this much mass, the black hole absorbs the matter around it and eventually uses up its own fuel [20].

This leads to a fascinating idea: as a quasar runs out of its energy source, it settles into a less violent state, which we observe as an active galaxy. As the galaxy evolves further, the fuel supply is further reduced, and the active galaxy evolves into the familiar elliptical and spiral galaxies. This theory implies that quasars are the ancestors of normal galaxies, including our own Milky Way [21]. Supporting this theory is evidence of energetic activity at the core of our galaxy, possibly the result of a massive black hole.

Although a quasar is luminous enough to be viewed from earth, accurate identification is a tedious process. When viewed in a telescope, quasars possess the same point-like appearance of stars [22]. Thus, they are exceedingly difficult to locate when juxtaposed with other stellar bodies.

Fortunately, quasars have a specific quality that facilitates their identification. They possess unique atomic spectra consisting of wide, redshifted emission lines [23]. Since these spectra are very different from those of stars, it is possible to distinguish a quasar from an ordinary star upon conducting data analysis.

The process of locating quasars begins at the computer lab, where candidates for further research are chosen. This is done by taking several variables into consideration: location, brightness, and the presence of reference stars. Software such as Red Shift, Palomar Sky Survey, and The Sky are used to obtain information regarding each variable.

Upon selecting candidates, CCD images are taken. By surveying the images, the quasars are further narrowed to one or two fields of view. These fields are at optimal positions for spectroscopy. The actual spectroscopy involves the use of the Self Guided Spectroscopy and the high-resolution, low-field-of-view CCD camera. Given the dimness of the quasars, it is necessary to use exposure times of 60 to 600 seconds when a spectrometer is used. It should be noted that it is rather tedious to line up quasars with the slit of the spectrometer due to their point-like stellar appearance.

Once the spectroscopy images have been taken, they must be calibrated, enhanced, and compared to the spectrum of mercury on Spectra. Consequently, the wavelength and intensity of the spectral lines are calculated. These estimates are subsequently entered in MatLab and graphed against one another. Afterwards, they are compared to the reference spectra of known quasars.

Our search for quasars began via the method described above. Two quasars, 1732+160 and 1553+159, were chosen as prime candidates for spectroscopy. However, given the

limitations of the instruments and the quasi-stellar appearance of quasars, attempts to obtain spectral data proved fruitless.

After several more unsuccessful attempts, a list of the ten brightest quasars visible from Earth was sought. Using this list, quasar 3C345, which possesses a variable magnitude of 15 to 17 as well as a detected redshift of .595, was selected.

Figure 6: Low-Resolution, High-Field-of-View Shot of 3C345

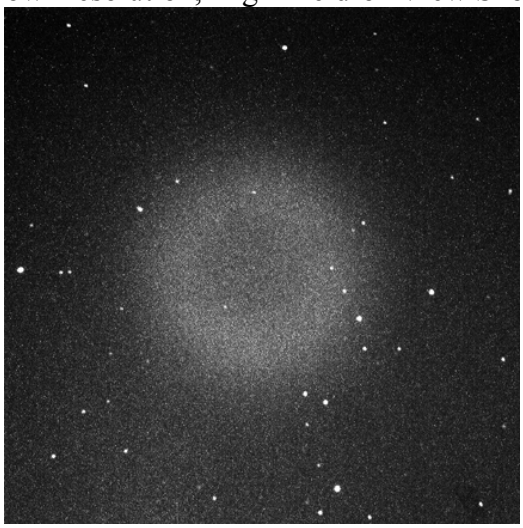

Spectroscopy was subsequently conducted on 3C345. Overall, broad absorption lines dominated the spectral graph. Strangely, only a few emission lines were detected.

Figure 7: Intensity vs. Wavelength Graph for Spectra of Quasar 3C345

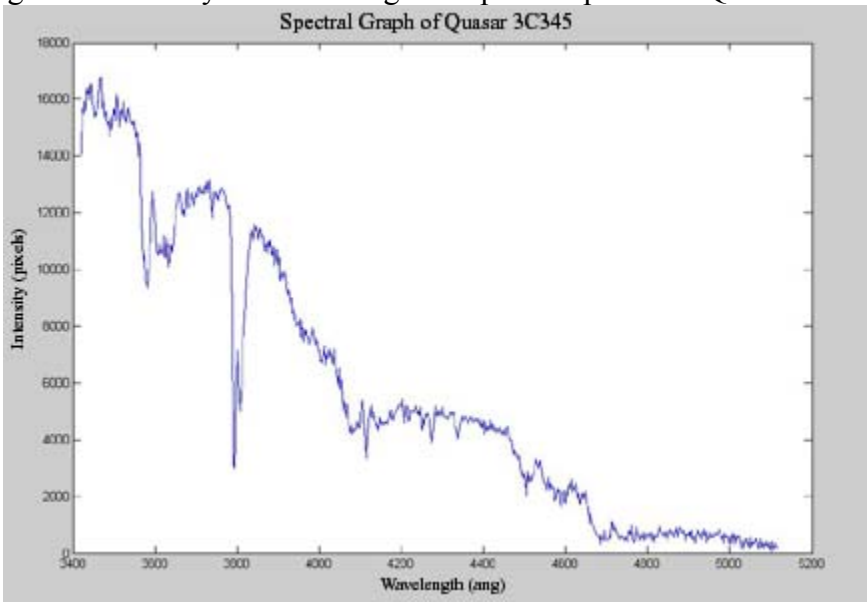

Figure 8: Mercury Calibration (below) and 3C345 Spectra (above)

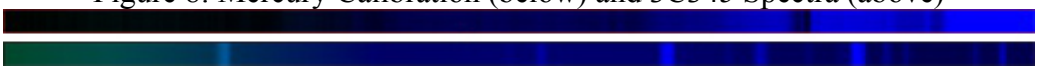

The broad absorption lines detected in the spectral graph of 3C345 are not typical of most quasars. However, the spectrum also bears no resemblance to known spectra of stellar bodies. This suggests that the spectral data possibly represents that of a galactic object or an atypical quasar.

Given the relatively high magnitude and low redshift detected in 3C345, it is highly probable that this quasar is nearby. If 3C345 is in fact within relatively close proximity to Earth, we perceive a much older object than the more remote quasars.

Considering the anomalous spectrum and the old age of 3C345 as well as theories suggesting that quasars are predecessors of active galaxies, it is conceivable that 3C345 is in the process of evolving into an active galaxy. Thus, the spectra produced by 3C345 would not be that of a typical quasar, but rather a combination of a quasar and an active galaxy.

Of course, proving this speculation sufficiently would require millions of years of observation, as the evolution of quasars occurs extremely slowly. Although there is no concrete proof that would validate our statements, the field of quasar research is based on probable speculations. Quasars remain the most baffling objects in the universe.

SPECTRA

The Vega project identified the elemental components of Vega by analyzing the absorption spectrum emitted by the star. By utilizing Spectra, MatLab, and the spectrograph, the specific gases which made up the star were determined.

Spectral analysis of stars is possible because every element in the universe has its own "spectral fingerprint" or unique pattern of dark lines in the absorption spectrum. An absorption spectrum is created when light is passed through a gas sample. The atoms of the gas absorb specific wavelengths of light corresponding to electron transitions between different energy levels. The light that passes through the opposite side of the gas sample forms an absorption spectrum, with dark bands on the spectrum corresponding to the wavelengths absorbed by the gas.

Stars, such as Vega, emit light. This light passes through the gases surrounding the star, and the gases absorb specific wavelengths of light, forming an absorption spectrum (Fig. 1). From the location of the dark bands in the absorption spectrum, it is possible to identify the elements in the star.

Figure 9: Absorption Spectrum [24]

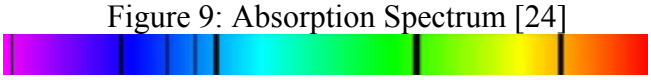

The Self Guided Spectrograph (SGS) was attached to the telescope camera and carefully calibrated by adjusting the focus and alignment of the device. This involved adjusting the SGS

slit to within two pixels of width on the computer screen and centering this slit in the computer window. Hexagonal Allen Wrenches were used to loosen and tighten screws in various locations in the SGS.

Once the SGS was focused, a calibration spectrum was collected from a mercury emission tube. The obtained spectrum was opened in Spectra and compared with an accepted mercury spectrum to determine if the lines matched (Fig. 2). After the collected spectrum's accuracy was confirmed, it was later used to calibrate the wavelengths of the Vega spectrum.

Figure 10: Comparison of Accepted and Obtained Hg Spectra

Figure 11: Star Centered on Slit

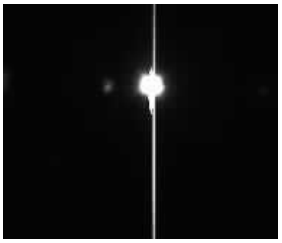

The SGS was then attached to the eyepiece of the Ritchey-Chrétien telescope. Using TheSky program, the telescope was slewed to the location of the star, Vega. Multiple exposures were taken and the position of the telescope was adjusted until the star was centered on the slit in the SGS (Fig. 3). A spectrum of Vega was then taken simultaneously with the calibration spectrum to provide a reference frame for the star's spectrum.

The obtained spectrum was then cropped in CCDOPS to the appropriate size for spectral analysis and was opened in the Spectra program. The Vega and calibration spectra were simultaneously displayed, and corresponding lines were identified. Spectra generated the wavelengths and intensities for all points on the Vega spectrum. Using MatLab, a plot of the intensity versus the wavelength of the spectrum was obtained.

The Vega spectrum was taken on August 1, 2002 with an exposure time of 66 seconds. The focal length was 270.mm and the alpha angle was 01.990 degrees. The telescope focus was on 3405 and the camera temperature was -4.4ºC.

The 4358 Å and 4046 Å lines of Hg were used to calibrate the Vega spectrum (Fig. 4).

Figure 12: Calibration and Vega Spectra

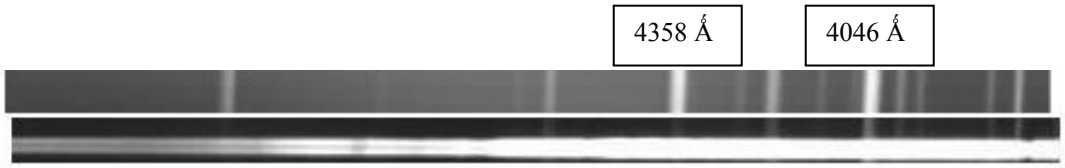

The following is a plot of intensity vs. wavelength generated in MatLab (Figure 13).

Figure 13: Wavelength vs. Intensity of Vega Spectrum

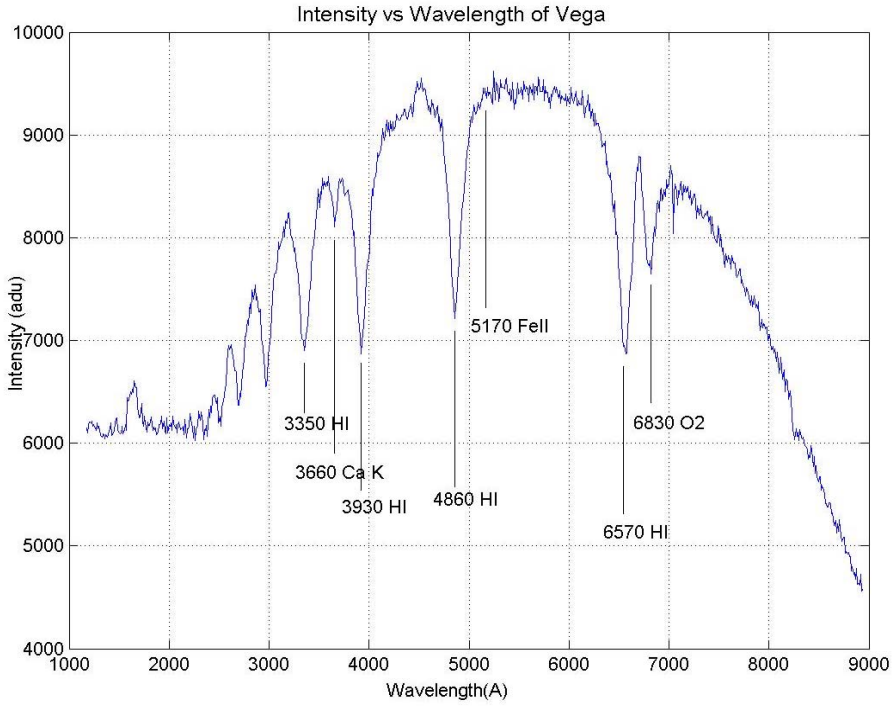

The bell shape of the graph was due to atmospheric conditions and camera sensitivity to specific wavelengths. Along the curve were sharp drops in intensity that corresponded to the dark lines of the absorption spectrum.

This spectrum was compared with the Balmer series, the absorption spectrum of hydrogen. Because hydrogen was so abundant in stars such as Vega, this absorption spectrum was very pronounced. The 6570 HI and 4860 HI lines on the Vega spectrum were corresponded with the hydrogen alpha line (6562 Å) and the hydrogen beta line (4861 Å)[25] of the Balmer series, recalibrating the spectrum over a wider wavelength range. These two lines were then used as reference lines for the rest of the Vega spectrum.

An accepted Vega spectrum was also obtained, and the collected Vega spectrum was compared with the accepted. Some labeled lines on the accepted spectrum were compared with those on the collected spectrum (Table 6).

Table 6 [26]
Comparison of Accepted and Experimental Wavelengths (Å)

Accepted	3889 HI	3934 Ca K	3970 HI	4861 HI	5169 FeII	6562 HI	6869 O2
Experimental	3350 HI	3660 Ca K	3930 HI	4860 HI	5170 FeII	6570 HI	6830 O2
Percent Error	-13.9 %	-6.96 %	-1.01 %	reference	0.0193 %	reference	-0.568 %

An average error of -4.48 % was obtained by averaging the errors of each line. The obtained errors were possibly due to light pollution, lack of repeated trials, and the inability of Spectra to fit a spectrum to a cubic scale. Because the predicted spectrum was a cubic function

and Spectra could only plot linearly, wavelengths farther away from the calibration lines became increasingly inaccurate.

A spectrum of Vega was successfully captured with the SGS. The Hg calibration spectrum, the Vega spectrum, and the Balmer series were matched, and wavelength and intensity were determined. After plotting the intensity vs. the wavelength of the spectrum and identifying the dark lines, a -4.48 % error was found between the lines of the accepted and experimental spectra. The spectrum of Vega was accurately obtained, and some of the star's elements (HI, Ca K, FeII, and O2) were correctly identified from position of the dark lines.

CONCLUSION

By using the telescope and other equipment to collect and analyze data, we were able to meet our research objectives. Our experiments ultimately yielded a range of dates for the creation of the Milky Way and an upper bound for the cosmological constant. We also acquired spectral data of a possible quasar and used the absorption spectrum of Vega to determine its elemental composition. Considering the constraints of time and equipment, reasonably accurate results were obtained. Further analysis of this data would have been facilitated by a longer research period and superior equipment. Despite all the difficulties encountered, we became proficient in using the observatory equipment—and thus successfully found answers in starlight.

REFERENCES

[1] http://www.depts.drew.edu/phys/astronomy/telescope.html

[2] http://www.northern-stars.com/tel_magnification.htm

[3] http://www.rcopticalsystems.com/overview.html

[4] http://www.sbig.com

[5] http://www.kodak.com/US/en/digital/dlc/book4/chapter2/glossaryC.shtml

[6] http://www.omegafilters.com/astro/bessel.html

[7] http://www.besoptics.com/html/body_schott_color_filters.html

[8] http://www.sbig.com/sbwhtmls/ccdacc.htm

[9] Holmes, Alan. *Operating Instructions for the Santa Barbara Instrument Group: Self Guided Spectrograph (SGS) and Spectra Analysis Software*. 2001.

[10] http://www.bisque.com/Products/TheSky/Databases.asp 1

[11] *TheSky Astronomy Software: User's Guide*. Version 5, Levels II, III, IV. Software Bisque. 1992-9.

[12] http://www.mathworks.com

[13] http://zebu.uoregon.edu/~soper/Stars/hrdiagram.html

[14] Collins, P.D.B., Mania A.D., Squires E.J. *Particle Physics and Cosmology*. Wiley Interscience. N.Y: 1989.

[15] Rindler, Wolfgang. *Essential Relativity: Special, General, and Cosmological*, 2nd edition. Springer-Verlag. N.Y: 1969.

[16] http://home.achilles.net/~jtalbot/-V1979/intro.html

[17] http://pegasus.phast.umass.edu/a100/handouts/quasar.html

[18] Chaisson, Eric and McMillan, Steve. *Astronomy Today*. Prentice Hall. Upper Saddle River, NJ: 1996. (p. 553)

[19] http://astro.princeton.edu/~library-/preprints/pop627.abs

[20] *Astronomy Today*, p. 554

[21] Snow, Theodore P. The *Dynamic Universe – An Introduction to Astronomy*. West Publishing Company. St. Paul, MN: 1985. (p. 515)

[22] http://imagine.gsfc.nasa.gov/docs/dict_gz.html#QSS

[23] http://www.ast.cam.ac.uk/~rgm/scratch/akarkut-/thesis/node5.html

[24] Cheng, Kwong-Sang., Chau, Hoi-Fung., and Lee, Kai-Ming. (2001). "Nature of the Universe." Retreived August 14, 2002, from Hong Kong Space Museum Web Site: http://bohr.physics.hku.hk/~nature/CD/regular_e/lectures/chap05.html.

[25] "Balmer Series." http://www.owlnet.rice.edu/~acobb/astr230/balmer_series_table.htm.

[26] Buil, Christian. (2002). "Index of /buil/us/vatlas." Retrieved August 9, 2002, from Spectroscopy, CCD, & Astronomy Web Site: http://www.astrosurf.com/buil/us/vatlas.